Arch. Metall. Mater. **65** (2020), 4, 1345-1350

DOI: 10.24425/amm.2020.133697

YOUNG-SANG CHO[1*], MINHO HAN[1], SEUNG HEE WOO[1]

ELECTROSPINNING OF ANTIMONY DOPED TIN OXIDE NANOPARTICLE DISPERSION FOR TRANSPARENT AND CONDUCTIVE FILMS

Stable dispersion of antimony-doped tin oxide nano-powder was prepared by wet attrition process by comminuting aggregated ATO nano-powder using the titanate coupling agent as a dispersant to form the chemisorbed layer on the particle surface. The feed solution of the ATO dispersion and PVP was prepared for electro-spun fibers on the glass substrate. The surface resistance of the fibrous ATO film after electrospinning for 30 minutes was in the order of 10^5 Ω/□, which is sufficient for anti-static coating. The optical transmittance of ATO fibers was confirmed by measuring the visible light transmittance.

Keywords: ATO nanoparticles, colloidal dispersion, electrospinning, transparent and conductive films

1. Introduction

Transparent and conductive oxides (TCOs) have been intensively studied because of their excellent electric conductivity and visible light transparency [1]. Thus, much effort has been exerted to apply TCOs in various areas, such as touch screen panels, electrode materials and EMI shielding films [2-4]. Although tremendous research related to TCOs focused on indium tin oxide (ITO), it is essential to replace ITO with other competitive materials since indium can be classified as a rare metal element. Thus, it is necessary to develop TCOs with economical prices and excellent physicochemical properties compa rable to ITO.

Antimony-doped tin oxide (ATO) has been studied because of its excellent chemical stability, visible light transparency and electric conductivity [5-6]. Synthesis of ATO has been conducted by doping tin oxide powder using antimony via chemical routes or direct fabrication of ATO powder by use of the sol-gel or co-precipitation method [7-9]. In order to fabricate the coating film of the ATO nanoparticles, synthesis and dispersion stabilization of the ATO nano-powder have been also studied using polar solvent as the dispersion medium or diethanolamine as dispersant in the aqueous medium [10,11]. However, it is necessary to develop stable dispersion of ATO nano-powder in organic solvents for electrospinning so as to fabricate the electro-spun ATO fibers, which have useful microstructure with one-dimensional conductive paths. Although one-dimensional ATO fibers can be synthesized using liquid precursors of Sb and Sn with proper polymer by electrospinning, the sol-gel or co-precipitation reaction can proceed during injection of the spinning solution for long intervals of time, which may cause clogging of the metallic nozzle [12]. In order to prevent this, the ATO nanoparticle dispersion with excellent dispersion stability can be adopted as raw material for electrospinning.

In this study, stable dispersion of the ATO nanoparticles in organic solvent was prepared by wet attrition milling using titanate coupling agent as the dispersant to prepare spinning solution. The factor affecting the secondary particle size was studied by changing the attrition time. Electrospinning was performed for deposition of the ATO nanofibers so as to prepare transparent and conductive film on glass subtrates. Visible light transmittance and surface resistance of the electro-spun film could be controlled by adjusting the milling time of the ATO nanoparticle dispersion and electrospinning time.

2. Experimental

Isopropyl tri (*N*-ethylenediamino) ethyl titanate (0.3 g) was mixed with ethanol (15.6 g) so as to prepare the dispersant solution. Commercial ATO nanopowder from Sigma-Aldrich (0.8 g) was mixed with ethanol (8.2 ml), followed by mixing the

[1] KOREA POLYTECHNIC UNIVERSITY, DEPARTMENT OF CHEMICAL ENGINEERING AND BIOTECHNOLOGY, 237 SIHEUNG-SI, GYEONGGI-DO 429-793, REPUBLIC OF KOREA

* Corresponding Author: yscho78@kpu.ac.kr

dispersant solution (3.6 g) and zirconia beads (3 ml) to the mixture for vibratory milling (Bottle Shaker, Model: Eg81960818Tv, Nodeco). The attrition process continued for fixed time intervals in order to measure the secondary particle size of the resulting dispersion after the sedimentation of zirconia beads.

The ATO nanoparticle dispersion (3 ml) was mixed with 3-ml PVP solution (1g/7 ml) under stirring, followed by feeding the solution to metallic nozzle (0.5 mm ID) using a syringe pump (10 μl/min). Electric fields, such as 12 kV, was applied using a high voltage power supply during electrospinning. The resulting composite fibers of the ATO and PVP were deposited on the glass substrate, followed by calcination at 500°C for five hours so as to prepare the ATO nanofibers using the box furnace. The surface resistance of the electro-spun ATO films was measured by applying the TLM method using a multi-meter [13].

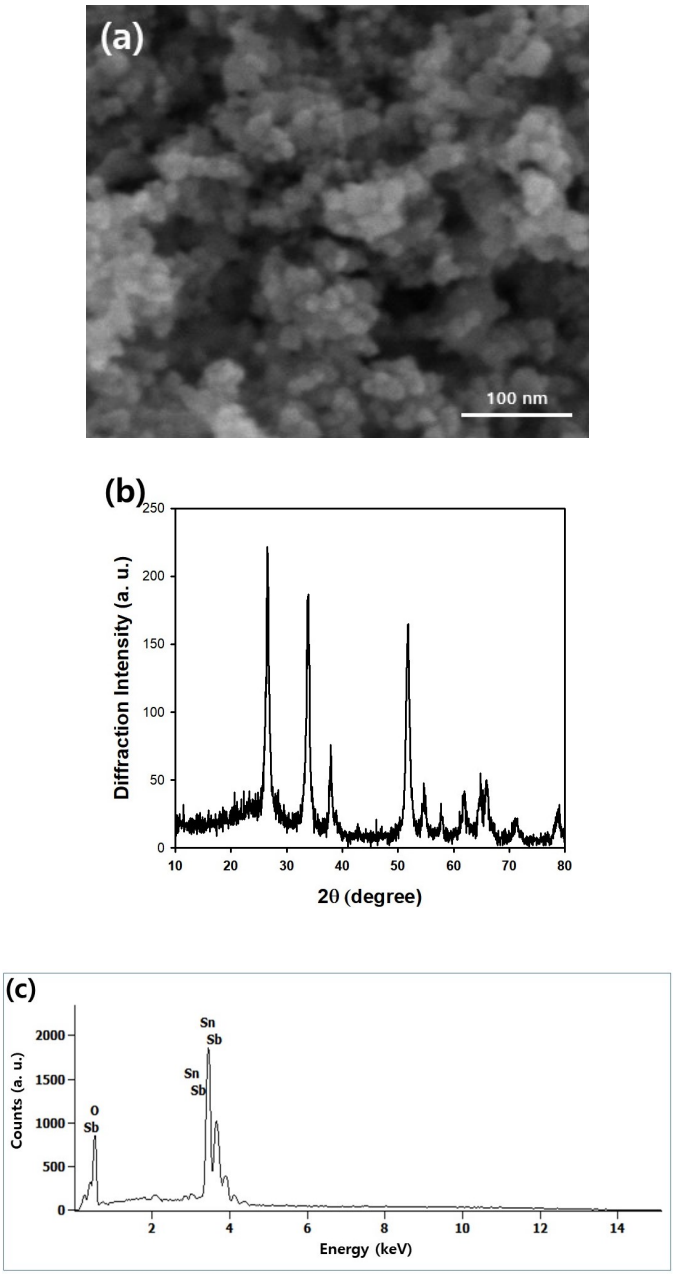

Fig. 1. (a) SEM image, (b) powder X-ray diffraction, and (c) EDS data of the ATO nano-powder

3. Results and discussion

Figure 1(a) comprises the SEM image of the commercial ATO nano-powder in this study, showing the primary particles with approximately 20 nm in diameter to form agglomerates. The crystallinity of the ATO nano-powder was analyzed by using XRD, and the result was as presented in Figure 1(b). The crystal structure of the nano-powder was confirmed as SnO_2 tetragonal structure, and the primary particle size, *t*, was calculated by using Scherrer's formula from FWHM of (100) peak in Figure 1(b) [14,15]. Here, the primary particle size was 47.97 nm, which is comparable to the size of the individual nanoparticles in the SEM image of Figure 1(a). The composition of the ATO nano-powder was also analyzed from the EDS data in Figure 1(c). The atomic ratio of the antimony to tin, [Sb]/[Sn] was 20.3%, which is close to the optimum value for maximum electrical conductivity of the ATO nano-powder [16].

Stable dispersion of the ATO nanoparticles was prepared from the aggregates of the ATO nano-powder by use of the wet attrition process. As presented schematically in Figure 2(a), the

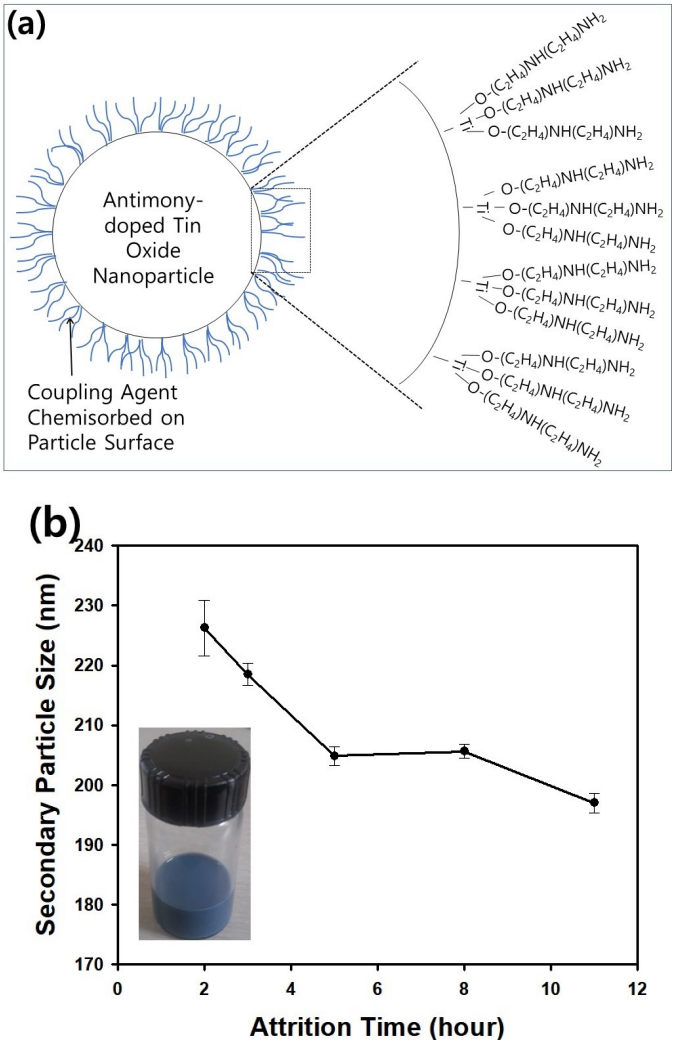

Fig. 2. (a) Schematic figure of chemisorption of titanate coupling agent on the ATO nanoparticle surface. (b) Size distribution of the ATO nanoparticle dispersion as a function of the attrition time. Inset image shows representative photograph of stable ATO nanoparticle dispersion

size reduction of the aggregates can be induced during the attrition process, and the chemisorption of the dispersing agent can be expected by alcoholysis reaction, resulting in steric stabilization of the ATO particles in the organic solvent. Figure 2(b) comprises the change of the secondary particle size as a function of the attrition time measured by light scattering. The size of particle dispersion decreased with increasing attrition time, indicating that the impact energy by zirconia beads induced the comminution of the aggregates of the ATO nano-particles. The secondary particle size of the ATO suspension could be decreased to approximately 200 nm, implying that more impact energy is required for further reduction of the size of the particle dispersion [17]. Although the vibratory frequency of the milling machine can be considered as a variable parameter, our wet attrition process was operated at a fixed frequency.

Figure 3(a) presents the SEM image of the composite fibers of the ATO and PVP with approximately 300 nm in thickness using stable dispersion of the ATO. The composition of the composite fibers was analyzed by using the FT-IR spectrometer, as displayed in the graph of figure 3(b). A strong absorption peak at 1,650 cm^{-1} originating from the carbonyl group of the PVP was observed as the characteristic peak before calcination [18]. The weight loss of the composite fiber was monitored with increasing temperature, and the TGA result was as presented in figure 3(c). Due to the thermal decomposition of the PVP from the composite fibers, the total weight decreased as temperature increased, and reached an equilibrium value of approximately 33% near 800°C. However, the calcination temperature in this study was determined as 500°C, since molten glass substrate may result in the decrease of electronic conductivity of the electro-spun ATO fibers when conventional soda lime glass is adopted [17]. For characterization of spinning solution, particle size distribution was measured, as displayed in Figure 3(d). The average particle size was measured as 1.62 and 0.72 μm for the samples after attrition for 2 and 6 hours, respectively, implying that aggregation of the nanoparticles occurred after mixing with PVP solution for preparation of the spinning solution. Though the average sizes were increased after formulation for spinning solution, the values were still smaller than the inner diameter of metallic nozzle (0.5 mm) for electrospinning.

Figure 4 presents the SEM images of the electro-spun ATO fibers fabricated after calcination at 500°C. In Figures 4(a) and 4(b), the attrition time of the ATO nanoparticle dispersion was three and five hours, respectively, before the preparation step

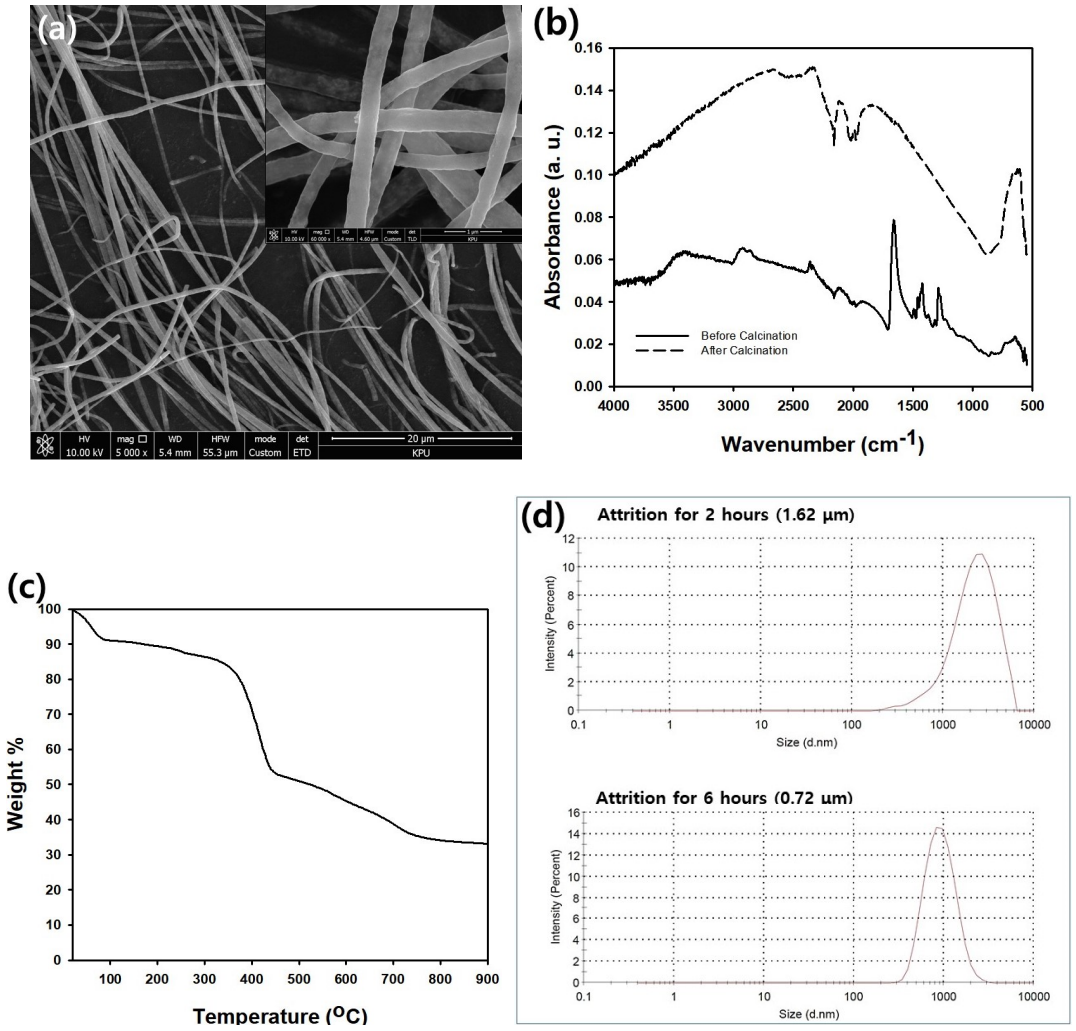

Fig. 3. (a) SEM image, (b) FT-IR spectrum, and (c) TGA result of the composite fibers of the ATO and PVP fabricated by electrospinning. (d) Size distribution of spinning solution prepared after attrition for 2 and 6 hours

of spinning solution. In these samples, fibrous materials could not be fabricated and short fragments were generated after heat treatment, implying that insufficient attrition time caused segregation of the ATO nanoparticles in the composite fibers because of the coarse particles in the ATO dispersion. Thus, fragmented ATO aggregates with rod-like morphologies could be observed after calcination for removal of the polymeric materials from the composite fibers, as displayed in Figures 4(a) and 4(b). On the contrary, continuous fibers could be obtained from the spinning solution prepared after comminution for six hours, as displayed in the SEM image of Figure 4(c), indicating that sufficient attrition time resulted in fibrous nano-structures of the ATO nanoparticles. Figure 4(d) comprises the surface resistance of the electro-spun ATO films as a function of attrition time of the ATO nano-particle dispersion. For the sample with attrition time of two hours, surface resistance of the ATO film was measured as a small value because of the large secondary particle size of dispersion, causing smaller contact resistance between the particles [4]. An increase of surface resistance was observed for the sample with attrition time of four hours because

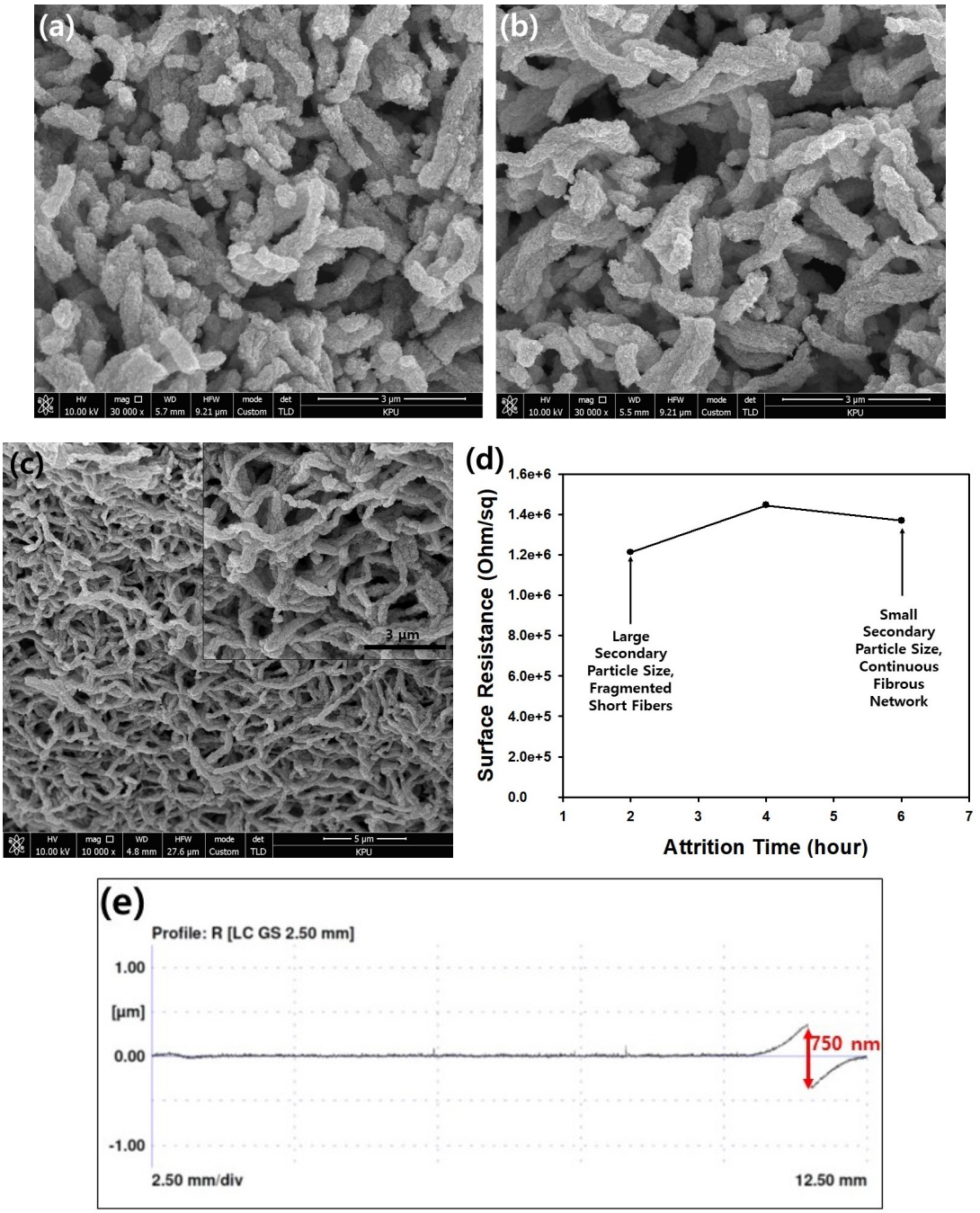

Fig. 4. SEM image of the conductive fibers fabricated by self-assembly of the ATO nanoparticles by the electrospinning. The feed solution during electrospinning was prepared by the wet attrition process for (a) three, (b) five and (c) six hours. (d) Surface resistance of the ATO films as a function of attrition time of the ATO nanoparticle dispersion. Electro-spinning was conducted for 10 minutes. (e) Surface roughness of electro-spun ATO fibers deposited partially on glass substrate. Spinning solution was prepared by attrition for 2 hours, and electro-spinning was carried out for 30 minutes

of the decrease of the secondary particle size, whereas resistance decreased when the attrition time increased to six hours. For prolonged attrition, such as six hours, the morphologies of the electro-spun ATO fibers changed as the continuous fibrous networks, causing conductive networks and decreased surface resistance, though the secondary particle size was smaller than other samples with short attrition times, as shown in Figure 4(d).

In this study, surface resistance of electro-spun ATO fiber film was estimated using 'TLM method' by measuring resistances from several points separated by fixed intervals on the film [13]. From the graph of resistance data as a function of separation distance, slope of regression line was multiplied by width of the film to obtain surface resistance. Though film thickness was not necessary during measurements of the surface resistance, we adopted indirect method to measure the film thickness by scanning the surface of glass substrate using roughness tester. Since only half of the substrate was deposited with electro-spun fibers, surface topography was suddenly changed from the region where electrospinning was applied, as displayed in Figure 4(e). Thus, film thickness of electro-spinning for 30 minutes could be determined as about 750 nm.

Figure 5(a) comprises the surface resistance of the electro-spun ATO films on the glass substrate as a function of the reciprocal of electrospinning time, after calcination of the films at 500°C. Because of the increase of the film thickness during prolonged electrospinning, the surface resistance decreased from the order of 10^6 to 10^5 Ω/□ with increasing spinning time, as shown in figure 5(b). Since film thickness of the electro-spun fibers increases as spinning time increases, the cross-sectional area of the conductive path becomes larger, causing a decrease and increase of surface resistance and conductivity, respectively, as shown in Figure 5(b). However, the value of the surface resistance was insufficient to obtain highly conductive films because of the intrinsic nature of the ATO nano-powder, which has inferior conductivity compared to other TCOs such as ITO. Thus, the electro-spun ATO films can be applied to anti-static or EMI shielding purposes rather than touch screen panels [19]. After spinning for 50 minutes, the surface resistance of the electro-spun ATO fiber film was measured as 6.45×10^4 Ω/□, indicating that the electrical resistance of the ATO film can be reduced to the comparable value of electro-spun ITO fibers reported by our previous research [17]. For comparison, the dip-coating of ATO nanoparticle dispersion was performed by the lifting-up of glass substrate with 0.06 mm/minute. After heat treatment at 500°C, the resulting dip-coated film showed surface resistance as 3.06×10^7 Ω/□, implying that electrospinning is a more efficient and practical manner for transparent and conductive film, compared to dip-coating with relatively long deposition time.

Temperature dependence of surface resistance was also studied by changing the calcination temperature of the electro-spun ATO film, as displayed in Figure 5(c). The order of resistance could be reduced from 10^5 to 10^4 Ω/□ by increasing the calcination temperature from 400-700°C. This is because organic materials, such as PVP and dispersant, can be removed more completely at higher temperatures. Partial sintering of the ATO nanoparticles in fibrous network can also be facilitated at higher temperatures, causing enhancement of electrical conductivity of the film. Since calcination at high temperatures requires high energy cost, we used 500°C as the heat treatment temperature for the electro-spun ATO fibers.

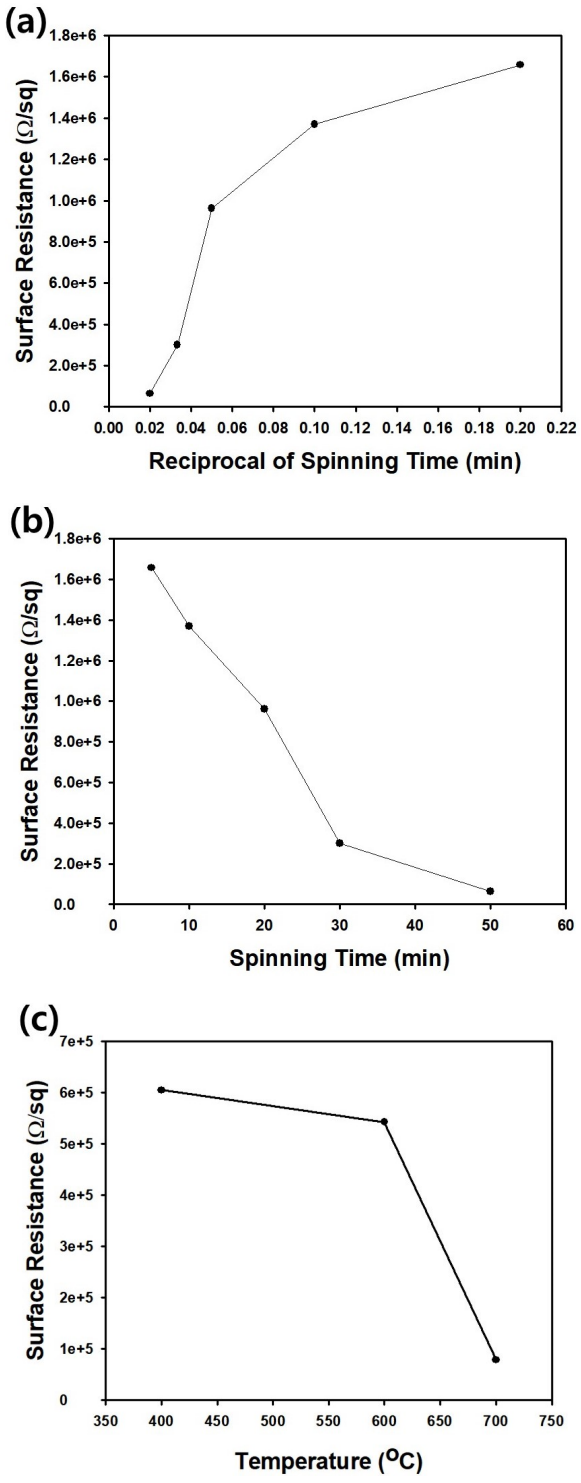

Fig. 5. Surface resistance of transparent and conductive film of the ATO fibers deposited on the glass substrate as a function of (a) the reciprocal of electrospinning, and (b) the spinning time, respectively. The feed solution was prepared by attrition for six hours. (c) Surface resistance of the electro-spun ATO film as a function of the heating temperature. Feed solution for electrospinning was prepared by attrition for two hours

Visible light transmittance of the electro-spun ATO fibers on glass substrate was measured as a function of wavelength of incident light, as displayed in Figure 6. Though significant difference between the spectrum was rarely observed from electrospinning for five and 10 minutes, further increase of spinning time resulted in decrease of the visible light transmittance due to the excess amount of the fiber network on the substrate, which blocked the transmission of light. For the coating film prepared for 30 minutes of electrospinning, light transmittance was slightly lower than 80% compared to bare glass, indicating that sufficient transparency could be guaranteed with good electrical conductivity. All spectra showed a slightly decreasing trend of transmittance near the UV region because of the bandgap of the ATO [20].

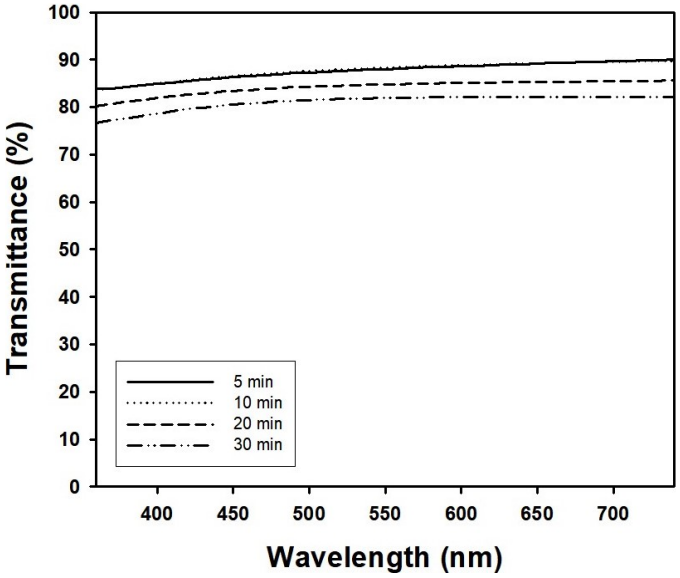

Fig. 6. Transmittance spectrum of the visible light of the electro-spun ATO fibers deposited on the glass substrate

4. Conclusion

In order to replace indium tin oxide with a low-cost TCO material, ATO nano-powder, was comminuted to prepare the stable dispersion of the ATO nanoparticles by use of the wet attrition process. The secondary particle size could be controlled in the range from 150-300 nm by adjusting the attrition time. The resulting stable dispersion could be used as feed solution for electrospinning by mixing with a PVP solution. Surface resistance of the coating film could be reduced to the order of 10^5 Ω/□ for 30 minutes of spinning, which is faster than the conventional dip-coating speed. Though electrical resistance increased with increasing spinning time, visible light transmittance decreased after prolonged electrospinning. However, transparency could be guaranteed with light transmittance higher than 90%.

Acknowledgments

This study was supported by the Basic Science Research Program through the National Research Foundation of Korea (NRF) funded by the Ministry of Science, ICT & Future Planning (NRF-2017R1C1B5017174) and the Priority Research Centers Program through the National Research Foundation of Korea (NRF) funded by the Ministry of Education (NRF-2017R1A6A1A03015562).

REFERENCES

[1] D.S. Ginley, C. Bright, MRS Bull. **25**, 15-18 (2000).
[2] K. Samadzamini, J. Frounchi, H.A. Veladi, AECE. **17**, 109-114 (2017).
[3] R.A. Afre, N. Sharma, M. Sharon , M. Sharon, Rev. Adv. Mater. Sci. **53**, 79-89 (2018).
[4] Y.-S. Cho, G.-R. Yi, J.-J. Hong, S.H. Jang, S.-M. Yang, Thin Solid Films **515**, 1864-1871 (2006).
[5] F. Kormos, I. Rotariua, G. Tolaib, M. Pávai, C. Romanc, E. Kálmán, Digest Journal of Nanomaterials and Biostructures **1** (3), 107-114 (2006).
[6] T. Zinchenko, E. Pecherskaya, D. Artamonov, AIMS Mater. Sci. **6** (2), 276-287 (2019).
[7] S.J. Jeon, J.J. Lee, J.T. Kim, S.M. Koo, J. Ceram. Proc. Res. **7** (4), 321-326 (2006).
[8] Y.-J. Lin, C.-J. Wu, Surface and Coatings Technology **88** (1-3), 239-247 (1997).
[9] J. Zhang, Y. Sun, J. Xu, Micro & Nano Lett. **14** (3), 254-258 (2019).
[10] K. Petters, P. Zeller, G. Stefanic, V. Skoromets, H. Nemec, P. Kuzel, D. Fattakhova-Rohlfing, Chem. Mater. **3**, 1090-1099 (2015).
[11] R. Ostermann, R. Zieba, M. Rudolph, D. Schlettwein, B.M. Smarsly, Electrospun antimony doped tin oxide (ATO) nanofibers as a versatile conducting matrix, Chem. Commun. **47**, 12119-12121 (2011).
[12] S. Santibenchakul, S. Chaiyasith, W. Pecharapa, Key Eng. Mater. **675-676**, 150-153 (2016).
[13] S.S. Cohen, Thin Solid Films **104**, 361-379 (1983).
[14] N. Zhao, L. Deng, D. Luo, S. He, P. Zhang, Int. J. Electrochem. Sci. **13**, 10612-10625 (2018).
[15] M.M. Munir, F. Iskandar, K.M. Yun, K. Okuyama, M. Abdullah, Nanotechnology **19** (14), 145603-145603 (2008)
[16] H.-J. Jeon, M.-K. Jeon, M. Lang, S.-G. Lee, Mater. Lett. **59** (14), 1801-1810 (2005).
[17] Y.-S. Cho, S. Jeong, S. Nam, J. Dispers. Sci. Tech., accepted for publication.
[18] R.P.D'Amelia, S. Gentile, W.F. Nirode, L. Huang, World. J. Chem. Edu. **4** (2), 25-31 (2016).
[19] H. Sun, X. Liu, B. Liu, Z. Yin, Mater. Res. Bull. **83**, 354-359 (2016).
[20] Y.N. Shieh, P.C. Hsieh, C.J. Chen, Adv. Mater. Res. **168-170**, 1670-1674 (2011).